Transdermal Drug Delivery by Jet Injectors: Energetics of Jet Formation and Penetration

Joy Schramm[1] and Samir Mitragotri[1,2]

Received July 19, 2002; accepted July 25, 2002

Purpose. Pressure-driven jets have been used for intradermal delivery of a variety of drugs. Despite their introduction into clinical medicine, variability and occasional bruising have limited their widespread acceptance. Although numerous clinical studies of jet injectors have been reported in the literature, surprisingly little is known about the mechanisms of jet penetration into the skin. In this article, we report results of our studies aimed at determining the dependence of drug delivery on jet velocity and diameter. These studies were performed using two experimental models, porcine skin and human skin. Our rationale for using two models was to explore the possibility of using porcine skin as a model for human skin.

Methods. Dermal penetration of jets possessing a range of diameters from 76 μm to 559 μm and a range of velocities from 80 m/s to 190 m/s was studied into human and porcine skin. Penetration was quantified using radiolabeled mannitol. Pressure and velocity of the jets were measured using a calibrated pressure transducer and high-speed photography.

Results. Penetration of the jet into the skin was determined by two main parameters, jet diameter and average jet velocity. Substantial variation in jet penetration into porcine skin was observed for skin pieces obtained from different anatomic locations. For porcine skin, a parabolic dependence of jet delivery on velocity and diameter was observed. The threshold velocity is suggested to be between 80 and 100 m/s for a jet diameter of 152 μm. Above the threshold velocity, the delivery increased for velocities up to 150 m/s, after which delivery decreased with increasing velocity. At a constant velocity of 150 m/s, jet delivery exhibited a maximum at a diameter of 152 μm. Results obtained with human skin were qualitatively similar but quantitatively different. The threshold velocity for jet penetration into human skin was comparable with that in porcine skin; however, the maxima observed in jet delivery into porcine skin with respect to jet velocity was not apparent for human skin over the range of velocities explored.

Conclusions. These studies offer a quantitative analysis of jet penetration into the skin.

KEY WORDS: jet injector; transdermal; skin; penetration; velocity; needle-free.

INTRODUCTION

Conventional needles offer the primary method for the delivery of macromolecular drugs. However, patient compliance with needle injection is low, especially for chronic prescriptions. With hopes of creating a painless injection method, jet injectors were developed in 1947, which produced a high-velocity jet that penetrated the skin (1). Since then, many devices have entered the market. However, almost 50 years since their invention, jet injectors have failed to replace conventional needles despite producing excellent drug bioavailability. Clinical studies suggest that this may be caused by the unreliability of the jet injection, including occasional drug pooling on the skin and bruising (2,3).

A jet injector produces a high-velocity jet (>100 m/s) that penetrates the skin and delivers drugs subcutaneously, intradermally, or intramuscularly without the use of a needle. The mechanism for the generation of high-velocity jets includes either a compression spring or compressed air. To date, commercial jet injectors have produced a single jet for drug delivery through an orifice ranging from 76 μm to 360 μm in diameter. However, the majority of the devices have an orifice diameter around 150 μm. Several studies have been reported on the use of jet injectors for drug delivery (4). However, the majority of the published research focuses on clinical trials. Several of these clinical studies have been reported on the use of jet injectors for insulin delivery (5). The bioavailability of insulin was found to be the same for jet injection as for the needle (6). Interestingly, the absorption rate of insulin delivered by jet injection has been shown to be higher than that by needles (6–8). The higher absorption rates have been attributed to a more diffuse pattern of drug delivered by jet injections compared to needles. The primary limitation of jet injectors has been inconsistency of penetration and pain.

Previous studies of jet injectors can be grouped into the following five categories: 1) pharmacokinetics (6–10); 2) tissue penetration and reaction (11–15); 3) pain and compliance (2,13,16–19); 4) safety (17,20); and 5) new clinical applications geared toward new drugs and injection sites (11,12,21). Very little published work has been reported on the mechanism of drug delivery by jet injections. Specifically, the dependence of the liquid jet penetration into the skin on two main jet parameters, diameter and velocity, has not been reported. In this work, we report results of our investigation of this issue.

MATERIALS AND METHODS

Jet Production

A commercial jet injector (Vitajet 3; Bioject Inc., Portland, OR, USA) was used to create jets from four different orifices (diameters of 76, 152, 229, and 559 μm) and various velocities in the range of 80–190 m/s. Vitajet 3 is a needleless, spring-powered jet injection system that is designed for insulin delivery. A picture of the device is shown in Fig. 1. The spring constant for this device was measured using an Instron universal testing machine (Instron 1123) and was found to be 17 kN/m. The velocity of the jet was controlled by adjusting the amount of spring compression as well as the piston friction. Two plastic rings are provided with the device for increasing the spring compression, which have thicknesses of 3 and 1.6 mm. The rings can also be used together to produce maximum spring compression. Vitajet 3 has disposable piston heads and clear thermoplastic nozzles. The nozzles are available in two different orifice diameters 152 and 178 μm. These nozzles were modified to increase the range of nozzle diameters studied in our experiments. Ruby orifice crystals (Sapphire Engineering, Pocasset, MA, USA) with diameters 76 and 229 μm were used in place of Vitajet orifice crystals. Above 229 μm, the crystal was removed and the thermoplas-

[1] Department of Chemical Engineering, University of California, Santa Barbara, California 93106.

[2] To whom correspondence should be addressed. (e-mail: samir@engineering.ucsb.edu)

0724-8741/02/1100-1673/0 © 2002 Plenum Publishing Corporation

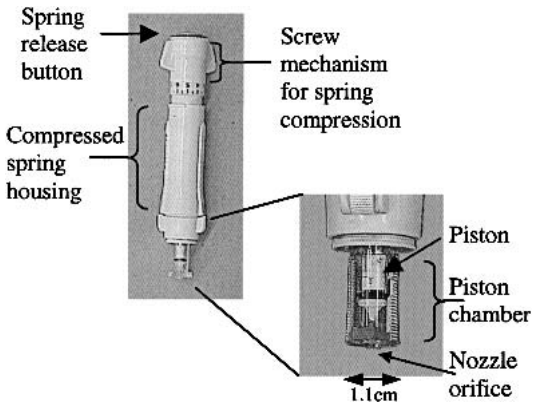

Fig. 1. Photographs of the jet injector, Vitajet 3, used in these experiments. The injector is driven by a compressed spring. The nozzle is made of clear thermoplastic and contains a sapphire orifice. An altered nozzle assembly was used to enable measurement of the pressure in the piston chamber. The Vitajet 3 nozzle was altered to accommodate the piezoelectric transducer with an outer diameter of 0.065 inches.

tic was drilled to the specified diameter. Thus, a wide range of nozzle diameters was investigated in this study.

Measurements of Jet Velocity and Piston Pressure

Pressure inside the chamber was measured using a calibrated piezoelectric transducer (Dynasen Inc., Goleta, CA, USA). The transducer possessed an outer diameter of 0.065", which allowed for minimal disturbance to the flow. The Vitajet 3 nozzle was altered in two ways to incorporate the pressure transducer. First, a hole was drilled in the nozzle so that the pressure transducer could be inserted. Second, a securing ring was added over the nozzle into which the transducer is threaded to hold it in place under high pressure. A charge integrator (Dynasen Inc.) comprising a 50 Ω resister and a 0.1 mF capacitor was used to facilitate pressure measurements. The charge integrator transforms the charge from the piezoelectric transducer into an output voltage, which is read by the oscilloscope (Tektronix, TDS 224). Each transducer was calibrated by Dynasen Inc. and showed a linear relationship between voltage and pressure. Output of the pressure transducer was collected via LabView with a time resolution of 2–100 μs, depending on the length of capture.

Velocity of the jet was determined by two methods and confirmed using theory. First, jet velocity was directly measured using a high-speed camera. A Kodak Ektapro Motion Analyzer 4540 (40500 frames per second maximum) was used for this purpose. The high-speed camera was used to capture the jet as a shadow illuminated by a white light source. Velocity of the jet was determined by the progression of the tip of the jet. This method is particularly applicable for determination of the initial velocity of the jet. Second, the average velocity of the jet was determined from the pressure profile. Specifically, as will be shown later, the formation and cessation of the jet is clearly visible in the pressure profile. This information can be used to determine the ejection time, $\tau_{ejection}$. Average jet velocity can be determined using the following equation

$$v_{jet}^{av} = \frac{Q}{A_{nozzle}\tau_{ejection}} \quad [1]$$

where A_{nozzle} is the cross-sectional area of the nozzle and Q is the total volume of liquid ejected. This method can be easily combined with penetration studies without the need for a high-speed camera and was used in the penetration experiments reported in this manuscript.

The calculated velocities were verified by comparison with Bernoulli's equation and fluid dynamical equations relating pressure to volumetric flow through the orifice. The theoretical maximum velocity of the jet for a given driving pressure in the nozzle is given by Bernoulli's equation. Utilization of this equation assumes that there are no frictional or turbulent energy losses in the orifice and nozzle. The resulting equation is given by

$$p \approx \frac{\rho v_{jet,\max}^2}{2} \quad [2]$$

where p is the pressure in the nozzle measured by the transducer, $v_{jet,max}$ is the theoretical maximum jet velocity, and ρ is the liquid density. This method can also be used to determine the maximum instantaneous velocity of the jet.

Flow through a small orifice causes both turbulent and frictional loses. In order to account for these losses, manufactures provided data from experiments that measure the flow of water through different diameter orifices with a pressure drop of one psi. The resulting equation includes the constant C_v, flow factor, which is a function of jet radius, r.

$$p = \left(\frac{\pi r^2 v_{\text{jet}}}{C_v(r)}\right)^2 \quad [3]$$

The measured pressure and calculated velocity are expected to follow this equation. C_v values for various orifices were provided by a manufacturer of similar orifices (0.00022, 0.00086, 0.0019, and 0.011 U.S. gallons of water per minute for one psi pressure drop for orifices possessing diameters of 76, 152, 229, and 559 μm, respectively, Bird Precision, Waltham, MA, USA).

Measurements of Drug Delivery into Skin

Delivery of a model drug, mannitol, into porcine and human skin by jet injection was measured. Experiments with porcine skin were performed using three different skin conditions: 1) freshly harvested, 2) previously frozen at −70°C, and 3) *in vivo*.

Experiments with Freshly Harvested Porcine Skin, Previously Frozen Porcine Skin, and Human Skin

Porcine skin used in all *in vitro* experiments was harvested from Yorkshire pigs and was excised immediately after sacrificing the animals. For one set of experiments, the skin was immediately used without freezing. In all other cases, the skin was cleaned to remove fat and subdermal tissues, and was frozen at −70°C until the time of experiments. All experiments were performed according to institutionally approved protocols. Human skin was procured through the National Disease Research Interchange.

At the time of jet injection, a piece of porcine or human skin was placed on a piece of wax paper and sealed on the

sides with medical tape. The skin was directly supported by the lab bench. A spacing ring was placed between the Vitajet 3 nozzle and the skin that raised the device 1 mm above the skin and insured no contact between the device and the skin at the time of injection. To assess mannitol delivery, a solution of ^{3}H-labeled mannitol (American Radiolabeled Chemicals, Inc., St. Louis, MO, USA) was prepared in deionized (DI) water at a concentration of 10 μCi/mL. A volume of 0.067, 0.096, or 0.126 mL of solution was loaded into the device. A jet was produced at various velocities and four diameters using strategies discussed earlier. To detect the amount of mannitol delivered across the skin, skin was placed on a Franz diffusion cell in some experiments and was injected using a jet injector. A sample of the receiver compartment of the diffusion cell was collected. Penetration of mannitol into the receiver compartment was rarely observed for porcine skin. Accordingly, we measured the amount of mannitol delivered into the skin. Once the injection was complete, excess fluid was removed from the top of the skin within one minute and the skin was placed in a scintillation vial. The skin was then dissolved in 2% sodium hydroxide solution (Solvable, Packard, Dowers Grove, IL, USA) at 65°C overnight. The amount of radiation in the skin was determined using liquid scintillation analysis [Tri-carb 2100TR, Packard). The scintillation cocktail used for these experiments was Ultima Gold (Packard).

Experiments with Porcine Skin in Vivo

In vivo experiments were performed within 10 min of sacrificing the animal. Although the animal had already been sacrificed at the time of experiment, the skin would have been alive and under tension and would mimic that on a living animal as far as jet penetration is concerned. In these experiments, a spacing ring was placed between the Vitajet 3 nozzle and the skin that raised the device 1 mm above the skin and a 10 μCi/mL solution of ^{3}H-labeled mannitol in DI water was injected using Vitajet. After the injection, the skin around the injection site was excised and assessed for mannitol using methods described above.

RESULTS AND DISCUSSION

Relationship of Jet Velocity with Pressure and Diameter

Figure 2 shows a typical pressure profile during ejection of 0.067 mL of DI water in air through a 152-μm nozzle (solid line). The pressure rises from the baseline level to a peak level of about 3900 psi (265 atm) in less than 0.5 ms. This step change indicates the release of the compressed spring and the subsequent beginning of the ejection. The step change is accompanied by oscillations in the pressure, including the abrupt peak pressure, which originate from the compressibility of the fluid. The true initial pressure of 2540 psi (173 atm) is determined using the center of the oscillations. There is a second step change that occurs 22 ms after the beginning of the ejection. This indicates the end of the ejection.

The duration of the jet determined using high-speed photography is consistent with the duration of the pressure pulse as defined by the time between the two step changes in pressure. Images of the jet captured during the initiation step were used to calculate the initial velocity of the jet, which was found to be about 150 m/s during the delivery of 0.067 mL of DI water (data not shown). The diameter of the jet was found to be comparable with the nozzle diameter. Minimal expansion of the jet was observed within 1.5 mm upon exiting the nozzle throughout most of each ejection. For this reason, we assumed the jet diameter to be the same as the nozzle diameter. Although high-speed pictures can be used to measure initial jet velocity, the determination of instantaneous velocities is difficult. Accordingly, we used average velocities determined from ejection time in our analysis. The average velocity determined from ejection time in Fig. 2 was also about 150 m/s, consistent with the velocity obtained from high-speed photography. We verified that the average velocities determined from the ejection time are also consistent with theory (Fig. 3). This figure shows average velocity as a func-

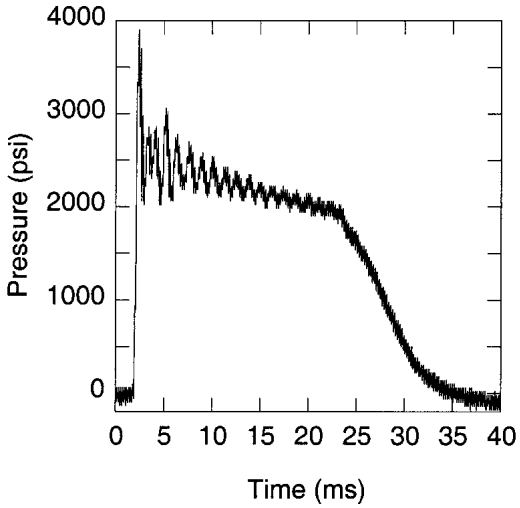

Fig. 2. Typical pressure curve for a 152-μm diameter nozzle from the jet injector Vitajet 3. The ejection begins at 2 ms at the first step change and ends at the second step change at 24 ms. The oscillations in pressure are caused by the compressibility of the fluid.

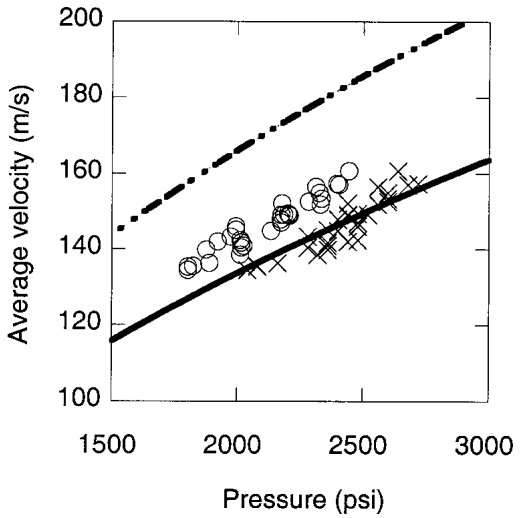

Fig. 3. Verification of calculated average velocity by the comparison of the velocity associated with the average pressure (○) and true initial pressure (X) to the maximum possible velocity for a given driving pressure expressed by the Bernoulli equation (dashed line) and Eq. 3 (solid line).

tion of pressure in the nozzle. Because the driving pressure of the jet is time-dependent, two pressure representations were used in Fig. 3. Open circles show the dependence of average velocity on the linear average of all pressures during the ejection, while crosses show the dependence of average velocity on the true initial pressure immediately after the ejection begins. The lines indicate theoretically calculated velocities. Dashed line corresponds to predictions of Bernoulli equation (Eq. 2) and solid line corresponds to predictions based on flow factor (Eq. 3). Experimentally determined velocities are lower than those determined from the Bernoulli equation (Eq. 2) and are near the expected pressure-velocity relationship of flow through an orifice (Eq. 3). This confirms that the calculated average velocities are physically consistent with the measured driving pressure.

A series of experiments were performed using various volumetric nozzle loadings between 0.067 and 0.126 mL. Figure 4 shows pressure profiles corresponding to injections of 0.067, 0.096, and 0.126 mL (profiles labeled A, B, and C, respectively). These experiments showed that the time duration of the jet increased proportionally with the volume of delivered liquid. Thus, the overall jet properties (pressures in the chamber and average jet velocity) are not affected by the amount of liquid loaded in the nozzle. In other words, a given nozzle produces a unique characteristic jet (at a fixed value of spring compression) (Fig. 4). Having established the relationship between relevant fluid dynamical properties of the jet, we sought to determine the dependence of jet penetration on these parameters.

Skin Model and Protocol Verification

Jet delivery into skin was studied using two experimental models, porcine skin and human skin. Porcine skin is a good model of human skin for testing diffusive permeability; however, this similarity may not extend to jet delivery, where the mechanical properties of skin might be important (22–26). Figure 5 compares jet delivery data into human (case A) and porcine (cases B and C) skin. Porcine skin used in cases B and C was obtained from two different anatomic locations (B, abdominal and C, dorsal). Within each case, different bars indicate different experimental conditions (closed bars, *in vivo*; hatched bars, *in vitro* frozen; and open bars, *in vitro* fresh). For each case, the skin tested under different experimental conditions was harvested from the same general anatomic location. Note that *in vivo* data for human skin (marked by an asterisk) were obtained from the literature (27) and data on freshly harvested human skin is not available. Data in Fig. 5 show that jet delivery into porcine and human skin *in vivo* and *in vitro* ($p > 0.45$) is comparable. Furthermore, there is no significant difference between jet delivery into previously frozen skin and freshly harvested skin ($p > 0.45$). However, there is a significant difference between jet delivery into human skin, porcine skin near the abdomen, and porcine skin near the back ($p < 0.001$). These differences in penetration are proposed to originate from the differences in the mechanical properties of the skin. To further evaluate the utility of porcine skin as a model for human skin, we measured the dependence of jet delivery on jet velocity and diameter.

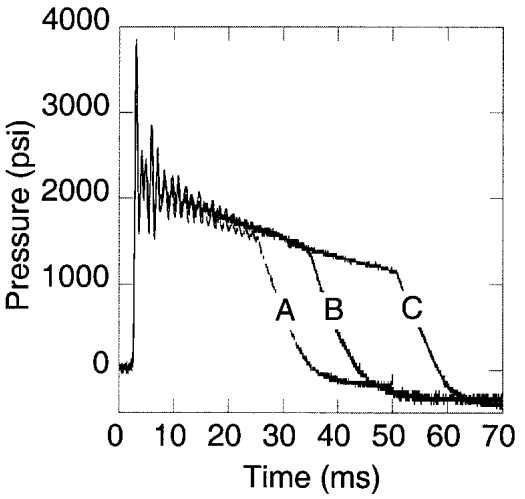

Fig. 4. Three different dispensing volumes of 0.067 mL (A), 0.096 mL (B), and 0.126 mL (C), produce coincident pressure curves where the ejection duration is proportional to the volume dispensed. This suggests that within this volume range a given nozzle (in this case a 152-μm diameter nozzle) produces a unique jet regardless of volumetric loading.

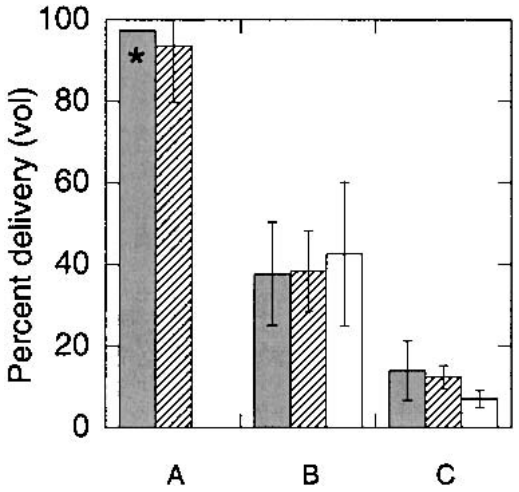

Fig. 5. Delivery of mannitol by jet injection into human (A), porcine abdominal (B), and porcine dorsal skin (C) using a 152-μm diameter nozzle at 177 m/s. There is a significant difference between each type of skin tested ($p < 0.001$). Within each case, different bars correspond to different experimental conditions: In vivo (closed bars), *in vitro* skin that has been stored at –70°C (hatched bars), and *in vitro* fresh skin (open bars) show no significant difference from one another ($p > 0.45$). The *in vivo* human data (*) is obtained from literature. Error bars correspond to one standard deviation ($n = 4$) (standard deviation of human *in vivo* data not available).

Dependence of Skin Penetration on Jet Parameters

Drug delivery by jet injection can be considered as two events: skin failure and convective flow though skin, a viscoelastic porous medium (28,29). We hypothesized that both events depend on two jet parameters, diameter and velocity, for the following reason.

The penetration of jets into skin is determined by the failure mechanics of the skin. Two different types of criteria can be considered for skin failure; one that compares the local stress induced by jet impact to a critical local stress and another that compares the energy density input to the skin to a critical energy density or work of fracture. Some progress has

been made in determining the work of fracture, G, and the critical local stress for human and porcine skin (30,31). Regardless of the exact values, both local stress and energy of the jet/skin system are dependent on jet velocity (v) and radius (r). Specifically, the local static stress of the impacting jet equals $\frac{1}{2}\rho v^2$ and acts on an area πr^2, whereas the kinetic energy of the impacting jet is given by, $\frac{1}{2}\rho(\pi r^2)v^3 t$ where t is the working time of the jet. After penetration into the skin, dispersion of the jet occurs by convective flow in porous media governed by Darcy's law (Eq. 4)

$$Q = \frac{K_D}{\mu} A \frac{\partial P}{\partial r} \qquad [4]$$

where, $\frac{\partial P}{\partial r}$ is the pressure gradient, A is the area over which the pressure gradient is acting, Q is the volumetric flow rate, and $\frac{K_D}{\mu}$, is the hydraulic conductivity, a ratio of "specific permeability" of the porous medium, K_D, to viscosity of the fluid, μ. The pressure gradient is created by the high impact pressure of the liquid jet on the skin and depends on the jet velocity and diameter. The area available for fluid transport, A, is the surface area of the hole created by the jet and is also likely to depend on the diameter of the impacting jet. Therefore, it is clear that various events in jet penetration are dependent on the two jet parameters, diameter and velocity. Consequently, the effect of changing jet diameter and velocity on drug delivery by jet injection was studied.

We first investigated the dependence of jet penetration on its velocity for both porcine and human skin. Figure 6A shows the percent of total ejected mannitol dose that penetrates into porcine skin as a function of velocity. For each experiment, a total of 0.067 mL of mannitol solution was ejected from the jet injector with a 152-μm diameter nozzle. The dependence of jet delivery on velocity is clouded by the variability in the experiments. Note that only a small variability (<7%) was observed in jet parameters, which suggests that the high variability in the delivery data is caused by the variability in jet/skin interactions. This variability may arise from many factors including variations in the material properties of the skin such as elastic modulus, work of fracture, and hydraulic conductivity, the hole size made by the jet, or variability in the angle between the jet and the skin. In order to elucidate the trend, the probability of delivery above a pre-set threshold was determined. This method is routinely used to analyze data possessing high variability. For example, if ten experiments were performed around a velocity $V \pm 10$ m/s and these experiments produced a range of percent deliveries from 0–40% then the probability of delivery above 20% at a velocity V would be the percentage of those ten experiments that produced deliveries above 20%. The data were divided into six velocity bins of width 20 m/s (80–100, 101–120, 121–140, 141–160, 161–180, and 181–190 m/s). Figure 6B shows the same data as in Fig. 6A but now shown in terms of the probability of delivering mannitol above thresholds of 10 to 90 volume percent. These thresholds are chosen for illustrative purposes. Statistical tests (z-test for proportions) were performed on the trend shown in Fig. 6B, which showed that the peculiar dependence of penetration on jet velocity, especially the existence of the peak, shown in Fig. 6B is indeed statistically significant (z-test, $z > 1.96$; 32,33). The dependence of delivery on velocity is qualitatively similar regardless of the choice of the threshold used for analysis. The data suggest that the threshold velocity for jet penetration is 80–100 m/s. Below this threshold, no significant mannitol delivery is expected (velocities below 80 m/s were not achievable with the current system). Beyond this graphically obtained threshold, mannitol delivery increased with increasing velocity until reaching a peak near 150 m/s and then decreased with increasing velocity. Some variability in the porcine experiments may be caused by the difference between skin pieces chosen for the experiments. To test that the trends were indeed caused by the velocity and diameter of the jet rather than skin pieces chosen Student t tests were performed on the resulting data. The trends were found to be statistically significant (z-test, $z > 1.96$) regardless of statistically different ($p < 0.05$) skin pieces.

Results of experiments on human skin are shown in Fig. 6C (closed circles), which also shows data on porcine skin for comparison (closed squares, reproduced from Fig. 6A). Threshold jet velocity required for penetration (as determined by extrapolation of data shown in Fig. 6C) is similar for human and porcine skin. However, unlike porcine skin, jet delivery into human skin increases monotonically in the range of velocities explored in this study. At any velocity, jet delivery into human skin is significantly higher than that into porcine skin. In the range of velocities explored, the highest delivery into human skin was about 92%.

The peak in mannitol delivery into porcine skin with jet velocity is likely to originate from the complex nature of the jet/skin interaction. Specifically, the percent volume delivery into the skin is the ratio of volumetric flow rate entering the skin to the volumetric flow rate out of the nozzle. At velocities below the threshold, the energy of the impacting jet would be lower than that required to rupture the skin and no penetration would be observed. Increasing jet velocity beyond the threshold results in an increase in rate of energy transfer as well as a greater increase in rate at which fluid is pushed into the skin compared with the rate at which fluid is ejected from the nozzle. This leads to an increase in percent volume delivery. However, at higher velocities for porcine skin, the percent delivery decreases with increasing velocity. The exact origin of this trend needs further investigation. Direct visualization of jet impact on the skin is necessary to assess the fundamental origin of this trend. By jet injecting a dyed solution into skin, we have verified that the majority of delivery occurs into or through the dermis for both skin types (data not shown).

The dependence of delivery on jet diameter was also investigated. Figure 7A shows the data for percent volume delivery into porcine skin at four different nozzle diameters (76, 152, 229, and 559 μm) at a velocity in the range of 140–160 m/s. These data were converted into probability of delivery above thresholds of 10 to 90 volume percent in the manner discussed previously. The results are shown in Fig. 7B. The probability of delivery for four nozzle diameters shows a peak in delivery for nozzle diameters between 152 to 559 μm (z-test, $z > 1.96$). Figure 7C shows jet delivery into human skin for the same four nozzle diameters (closed circles). Data on porcine skin is also shown for comparison (closed squares, reproduced from Fig. 7A). Once again, delivery into human skin is significantly greater than that into porcine skin. The overall dependence of jet delivery on nozzle diameter is similar for porcine and human skin.

The maximum observed in jet penetration with respect to

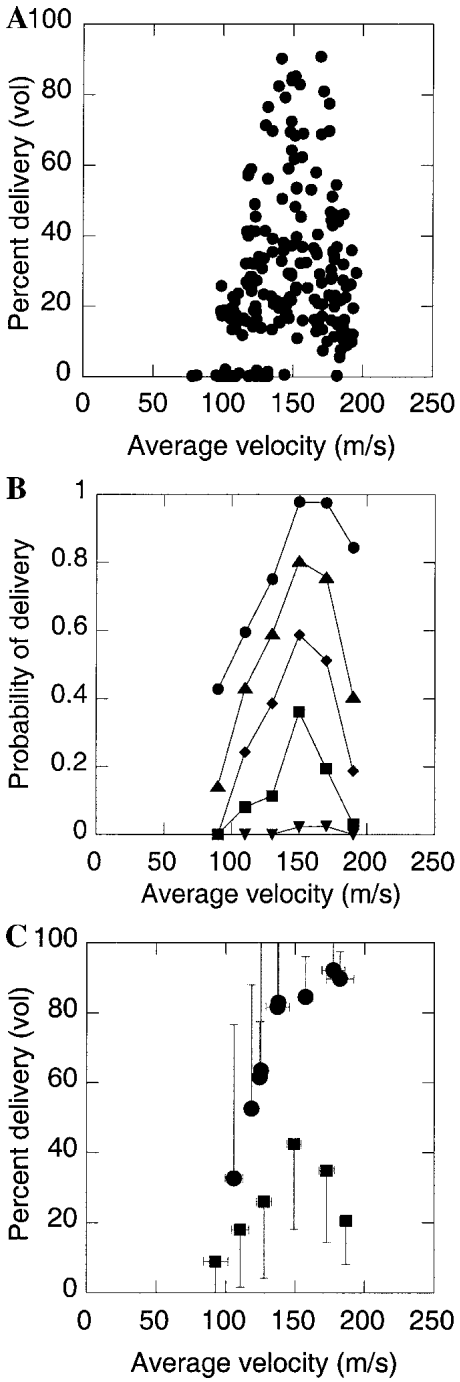

Fig. 6. (A) Percent volume delivery of mannitol by jet injection through a 152-μm diameter nozzle into porcine skin. These raw data for the velocity range 80–190 m/s show high variability that is attributed solely to the jet/skin interaction (n = 100). (B) Probability of delivery of mannitol by jet injection above thresholds of 10% (●), 20% (▲), 30% (♦), 50% (■), and 90% (▼) volume delivery. These are the same data as in Figure 6A now presented in terms of probabilities. The data were divided in velocity bins of 20 m/s width within which the probabilities of delivery were determined. The choice of delivery thresholds is arbitrary and only done to show the resulting significant statistical trend when the data is treated in terms of probabilities. The peak in delivery is statistically significant. (C) Average percent delivery of mannitol by jet injection through a 152-μm diameter nozzle into human (●) and porcine (■) skin. The error bars shown are one standard deviation. The magnitude of the delivery into human skin is higher than into porcine skin (n = 5–19 for each human skin data point).

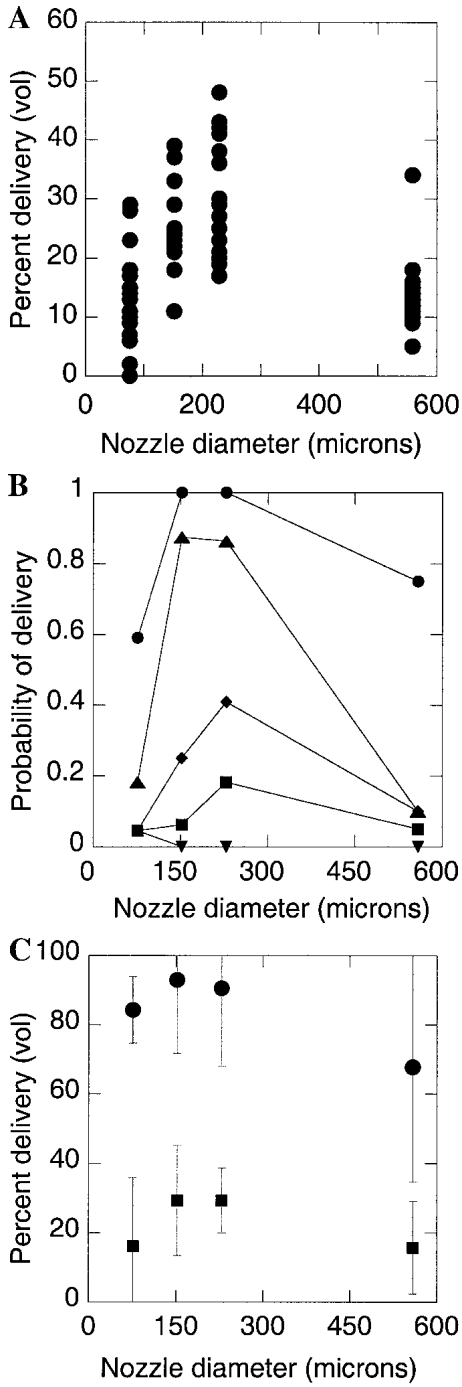

Fig. 7. (A) Percent volume delivery of mannitol into porcine skin by jet injection at four different nozzle diameters: 76, 152, 229, and 559 μm. The average velocity was nearly the same at each of the nozzle diameters between 140–160 m/s (n = 80). (B) Probability of delivery of mannitol by jet injection at four different nozzle diameters (76, 152, 229, and 559 μm) above arbitrary thresholds of 10% (●), 20% (▲), 30% (♦), 40% (■), and 90% (▼) volume delivery. These are the same data as in (A) now presented in terms of probabilities. This shows a peak in delivery occurs between 152 to 559 μm in diameter. (C) Average percent delivery of mannitol by jet injection at four different nozzle diameters: 76, 152, 229, and 559 μm into human (●) and porcine (■) skin. The porcine delivery data are the same data as presented in (A) and (B). The error bars shown are one standard deviation. The magnitude of the delivery into human skin is higher than into porcine skin but results in the same parabolic trend (n = 20 for each human skin data point).

jet diameter is very peculiar. As the jet diameter increases, the rate of energy transfer to the skin also increases thereby possibly leading to an increase in delivery. However, if the rate at which the fluid is ejected from the nozzle exceeds the rate at which fluid can be forced into the skin, the overall fraction of delivery may decrease. Future studies should focus on understanding the physical origin of these trends as well as assessing whether these trends depend on the jet and skin parameters not controlled in this study.

CONCLUSIONS

The data presented in this article show that penetration of a liquid jet into skin depends on jet diameter and jet velocity. For porcine skin, jet delivery exhibits an optimum with respect to both jet parameters. The threshold velocity necessary for skin penetration for a jet diameter of 152 μm is suggested to be between 80–100 m/s. Beyond this value, mannitol transport in porcine skin increases until a maximum at 150 m/s followed by a decrease in delivery. A peak in mannitol delivery was also observed with respect to jet diameter at a velocity range between 140–150 m/s. For human skin, jet delivery increases monotonically with respect to jet velocity, while it exhibits an optimum with respect to jet diameter similar to that observed for porcine skin.

ACKNOWLEDGMENTS

This work was supported by Materials Research Laboratory at University of California, Santa Barbara and Centers for Disease Control and Prevention. Authors thank Dr. Charest of Dynasen Inc. for helpful discussions and Ocean Feniger and Haydee Rodriguez for assistance.

REFERENCES

1. F. H. J. Figge and D. J. Barnett. Anatomic evaluation of a jet injection instrument designed to minimize pain and inconvenience of parenteral therapy. *Am. Practicioner* **3**:197–206 (1948).
2. U. Schneider, R. Birnbacher, and E. Schober. Painfulness of needle and jet injection in children with diabetes mellitus. *Eur. J. Pediatr.* **153**:409–410 (1994).
3. G. Wijsmuller and D. E. Snider Jr. Skin testing: A comparison of the jet injector with the mantoux method. *Am. Rev. Respir. Dis.* **112**:789–798 (1975).
4. B. G. Weniger. (www.cdc.gov/nip/dev/JetinjeBib.pdf, 2000), vol. 2001.
5. F. S. Perkin. Jet Injection of insulin in treatment of diabetes mellitus. *Proc. Diabetes Assoc.* **10**:185–199 (1950).
6. A. Consoli, F. Capani, G. La Nava, A. Nicolucci, G. P. Prosperini, G. Santeusanio, and S. Sensi. Administration of semisynthetic human insulin by a spray injector. *Bollettino - Societa Italiana Biologia Sperimentale* **60**:1859–1862 (1984).
7. J. Halle, J. Lambert, I. Lindmayer, K. Menassa, F. Coutu, A. Moghrabi, L. Legendre, C. Legault, and G. Lalumiere. Twice-daily mixed regular and NPH insulin injections with new jet injector versus conventional syringes: Pharmacokinetics of insulin absorption. *Diabetes Care* **9**:279–282 (1986).
8. G. Kerum, M. Profozic, G. Skrabalo, and Z. Skrabalo. Blood glucose and free insulin levels after the administration of insulin by conventional syringe or jet injector in insulin treated type 2 diabetics. *Horm. Metab. Res.* **19**:422–425 (1987).
9. F. K. Bauer, B. Cassen, E. Youtcheff, and L. Shoop. Jet Injection of Radioisotopes—a clinical study comparing needle and jet injection of I_{131}, K_{42}, and Na_{24}. *Am. J. Med. Sci.* **225**:374–378 (1953).
10. L. Jovanovic-Peterson, S. Sparks, J. P. Palmer, and C. M. Peterson. Jet injected insulin is associated with decreased antibody production and postprandial glucose variability when compared with needle-injected insulin in gestational diabetic women. *Diabetes Care* **16**:1479–1484 (1993).
11. R. M. Seyam, L. R. Begin, L. M. Tu, S. B. Dion, S. L. Merlin, and G. B. Brock. Evalution of a no-needle penile injector: A preliminary study evaluating tissue penetration and its hemodynamic consequences in the rat. *Urology* **50**:994–998 (1997).
12. N. Inoue, D. Kobayashi, M. Kimura, M. Toyama, I. Sugawara, S. Itoyama, M. Ogihara, K. Sugibayashi, and Y. Morimoto. Fundamental investigation of a novel drug delivery system, a transdermal delivery system with jet injection. *Int. J. Pharmaceutics* **137**: 75–84 (1996).
13. M. L. Cohn, R. A. Hingson, J. V. Narduzzi, and J. M. Seddon. Clinical experience with jet insulin injection in diabetes mellitus therapy: A clue to the pathogenesis of lipodystrophy. *Ala. J. Med. Sci.* **11**:265–272 (1974).
14. A. K. ElGeneidy, A. A. Bloom, J. H. Skerman, R. E. Stallard. Tissue reaction to jet injection. *Oral Surg. Oral Med. Oral Pathol.* **38**:501–511 (1974).
15. C. R. Bennett, R. D. Mundell, and L. M. Monheim. Studies on tissue penetration characteristics produced by jet injection. *J. Am. Dental Assoc.* **83**:625–629 (1971).
16. P. Bareille, M. MacSwiney, A. Albanese, C. D. Vile, and R. Stanhope. Growth hormone treatment without a needle using the Preci-Jet 50 transjector. *Arch. Dis. Child.* **76**:65–67 (1997).
17. G. E. Theintz and P. C. Sizonenko. Risks of jet injection of insulin in children. *Eur. J. Pediatr.* **150**:554–556 (1991).
18. I. Lindmayer, K. Menassa, J. Lambert, A. Moghrabi, L. Legendre, C. Legault, and M. Letendre. J. Halle. Development of new jet injector for insulin therapy. *Diabetes Care* **9**:294–297 (1986).
19. A. H. Kutscher, G. A. Hyman, E. V. Zegarelli, J. Dekis, and J. D. Piro. A comparative evalution of the jet injection technique (hypospray) and the hypodermic needle for the parenteral administration of drugs: A controlled study. *Am. J. Med. Sci.* **244**:418–420 (1962).
20. J. P. Price, D. F. Kruger, and L. D. Saravolatz. F. W. Whitehouse. Evaluation of the jet injector as a potential source of infection. *Am. J. Infect. Control* **17**:258–263 (1989).
21. K. Sugibayashi, M. Kagino, S. Numajiri, N. Inoue, D. Kobayashi, M. Kimura, M. Yamaguciii, and Y. Morimoto. Synergistic effects of iontophoresis and jet injector pretreatment on the in-vitro skin permeation of diclofenac and angiotensin. *J. Pharm. Pharmacol.* **52**:1179–1186 (2000).
22. T. K. Das Gupta, S. G. Ronan, C. W. Beattie, A. Shilkaitis, and M. S. J. Amoss. Comparative histopathology of porcine and human cutaneous melanoma. *Pediatr. Dermatol.* **6**:289–299 (1989).
23. L. W. Weber. The penetration of 2,3,7,8-tetrachlorodibenzo-p-dioxin into viable and non-viable porcine in vitro. *Toxicology* **84**:125–140 (1993).
24. U. Wollina, U. Berger, H. Stolle, H. Schubert, and M. Zieger. H. C., D. Schumann. Tissue expansion in pig skin—a histochemical approach. *Anat. Histol. Embryol.* **21**:101–111 (1992).
25. D. Marro, R. H. Guy, and M. B. Delgado-Charro. Characterization of the iontophoretic permselectivity properties of human and pig skin. *J. Control. Release* **70**:213–217 (2001).
26. W. Meyer. Comments on the suitability of swine skin as a biological model for human skin. *Hautarzt* **47**:178–182 (1996).
27. D. L. P. D. Bremseth and F. M. D. Pass. Delivery of insulin by jet injection: Recent observations. *Diabetes Technol. Ther.* **3**:225–232 (2001).
28. J. C. Barbenel and J. H. Evans. The Time-Dependent Mechanical Properties of Skin. *J. Invest. Dermatol.* **69**:318–320 (1977).
29. M. S. Christensen, C. W. Hargens III, S. Nacht, and E. H. Gans. Viscoelastic properties of intact human skin: Instrumentation, hydration effects, and the contribution of the stratum corneum. *J. Invest. Dermatol.* **69**:282–286 (1977).
30. J. Ankersen, A. E. Birkbeck, R. D. Thomson, and P. Vanezis. Puncture resistance and tensile strength of skin stimulants. *Proc. Inst. Mech. Eng. Part H - J. Eng. Med.* **213**:493–501 (1999).
31. B. P. Pereira, P. W. Lucas, and T. Swee-Hin. Ranking the fracture toughness of thin mammalian soft tissues using the scissors cutting test. *J. Biomech.* **30**:91–94 (1997).
32. D. J. Sheskin. In: T. Pletsche (ed.) *Handbook of Parametric and Nonparametric Statistical Procedures*, pp. 226–331, CRC Press, Boca Raton, Florida, 1997.
33. D. Freedman, R. Pisani, and R. Purves. In: *Statistics,* pp. 437–461. W. W. Norton & Company Inc., New York, 1978.